Zeitschrift: Schweizerische mineralogische und petrographische Mitteilungen = Bulletin suisse de minéralogie et pétrographie

Band: 67 (1987)

Heft: 1/2

Artikel: Derivation and application of a solution model for calcic garnet

Autor: Engi, Martin / Wersin, Paul

DOI: https://doi.org/10.5169/seals-51587

SCHWEIZ. MINERAL. PETROGR. MITT. 67, 53-73, 1987

Derivation and application of a solution model for calcic garnet*

by *Martin Engi*[1] and *Paul Wersin*[2]

Abstract

Contrary to earlier studies, the thermodynamic solution behaviour derived here for calcic garnet is strongly nonideal. Published experimental data on grossular-andradite ($Ca_3Al_2Si_3O_{12}$-$Ca_3Fe_2Si_3O_{12}$) are carefully analyzed and are shown to be well represented by an asymmetric (subregular) Margules solution with

$W_{G,gro} = +12.906\ kJ\,mol^{-1}$ $\quad W_{V,gro} = -2.60\ cm^3mol^{-1}$
$W_{G,and} = -46.910\ kJ\,mol^{-1}$ $\quad W_{V,and} = -0.55\ cm^3mol^{-1}$

Whereas lattice strain effects cause the positive deviation from ideality in grossular-rich grandite, Al-Fe^{3+} ordering is thought responsible for the pronounced negative deviation. Theoretical models of both these proposed structural mechanism yield energetic effects in approximate agreement with the interaction parameters found by purely thermodynamic analysis. The consequences of the solution model are further supported by recent crystallographic data on exsolved and anisotropic calcic garnets.

Petrological uses of the solution model include an update of the skarn geothermometer based on the equilibrium

$$\underset{\text{garnet}}{Ca_3Al_2Si_3O_{12}} + \underset{\text{quartz}}{SiO_2} = \underset{\text{anorthite}}{CaAl_2Si_2O_8} + \underset{\text{wollastonite}}{2\,CaSiO_3}$$

and extensions thereof, which limit the T-X(CO_2) conditions of equilibration for common calc-silicate and skarn assemblages. Comparison of this thermometer with the calcite-dolomite thermometer from alpine skarn occurrences and selected examples from the literature proved favorable.

Keywords: Solution model, grossular-andradite, garnet, geothermometry, Alps.

1. Introduction

Low-variance assemblages in metamorphic calc-silicate rocks, including skarns, typically contain grandite, a garnet variety rich in the components grossular ($Ca_3Al_2Si_3O_{12}$) and andradite ($Ca_3Fe_2Si_3O_{12}$). At low metamorphic grade a few mole percent of hydro-garnet components are typical (e.g. COOMBS et al., 1977; HUCKENHOLZ and FEHR, 1982), especially in quartz-undersaturated assemblages. Nearly binary solutions between grossular and andradite are common (Fig. 1) at high metamorphic grade, except for Mn-rich bulk compositions and certain skarns which equilibrated under very reduced conditions (see e.g. SHIMAZAKI, 1977; NEWBERRY, 1983). In calc-silicate gneisses from regionally or contact-metamorphosed terrains, a variety of parageneses include grandite for which the mole fractions $X_{gro} + X_{and}$ typically add to 0.95 or greater; almandine, pyrope, spessartine and Ti-components contribute the remainder (SOBOLEV, 1964; EINAUDI and BURT, 1982). Compared with garnet varieties from pelitic or mafic rocks, calc-silicate garnets are thus compositionally simple. For these reasons, the thermodynamic characteristics of grandites, especially their detailed

* Dedicated to Professor Ernst Niggli on the occasion of his 70th birthday.

[1] Mineralogisch-Petrographisches Institut, Universität Bern, Baltzerstrasse 1, CH-3012 Bern.
[2] Institut für Mineralogie und Petrographie, ETH-Zentrum, CH-8092 Zürich.

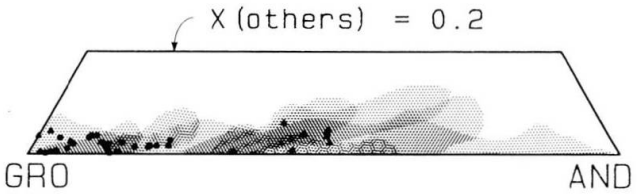

Fig. 1 Range of garnet compositions in quartz-saturated calc-silicate assemblages equilibrated at temperature higher than approximately 300 °C. Molar abundances of components beside GRO(ssular) and AND(radite) are combined in "others". Data compiled from literature (shaded areas) and present study (single symbols).

activity-composition relations, would seem of particular petrological interest.

Yet pertinent investigations of grandite are surprisingly scarce, when compared to the attention chemically more complex solutions of the pyralspite series have received (e.g. NEWTON and HASELTON, 1981; HODGES and SPEAR, 1982; GANGULY and SAXENA, 1984, and references therein).

Furthermore, previous studies of the mineralogy of grandite, its thermodynamics and stable phase relations, yield an inconsistent picture and, in part, derive opposing conclusions (e.g. BIRD and HELGESON, 1980; WASSERMANN et al., 1982).

In the present paper we analyze the available experiment phase equilibrium and crystal-chemical data with the intent of first identifying and resolving inconsistencies and then deriving from the accepted data set a solution model for calcic garnet, especially for the grossular-andradite binary. Theoretically derived coefficients for a multicomponent activity model will be presented subsequently.

By way of example, the newly developed solution model is then applied to interpret mineral equilibria typical of calc silicate paragenesis. The petrogenesis of assemblages involving grandite and plagioclase is explored and a new formulation of the garnet-plagioclase-wollastonite-quartz geothermometer is suggested. Applications are based primarily on new microprobe data of suitable assemblages from several localities in the Alps. In addition, selected examples from the literature are discussed, with the aim of characterizing their P-T-X(CO_2) conditions of metamorphism.

2. Review and critique of previous work

2.1. EXPERIMENTAL DATA

Experimental stability relations of calcic garnets, as well as their thermochemical properties have been investigated primarily for the endmembers grossular (phase equilibria: YODER, 1950; HAYS 1966; NEWTON, 1966; HARIYA and KENNEDY, 1968; BOETTCHER, 1970; STORRE, 1970; GORDON and GREENWOOD, 1971; HOSCHEK, 1974; SHMULOVICH, 1974, 1977; HUCKENHOLZ, 1974; HUCKENHOLZ et al., 1975; WINDOM and BOETTCHER, 1976; WOOD, 1978; GOLDSMITH, 1980; GASPARIK, 1984; KERRICK and GHENT, 1984. Calorimetry: PERKINS et al., 1977; KOLESNIK et al., 1979; KRUPKA et al., 1979; WESTRUM et al., 1980) and, to a much lesser extent, andradite (phase equilibria: HUCKENHOLZ and YODER, 1971; GUSTAFSON, 1974; LIOU, 1974; SUWA et al., 1976; TAYLOR and LIOU, 1978).

Much less attention has been devoted to the stability of intermediate grandite; for example, no calormetric data are available to date. HOLDAWAY (1972) and HUCKENHOLZ et al. (1981) measured the composition of grandite equilibrated in the presence of anorthite, wollastonite, and silica (quartz or tridymite). PERCHUK and ARANOVICH (1979) studied the Al-Fe^{3+} exchange equilibrium between grandite and aqueous chloride solutions. Garnet equilibria from two other experimental studies (HOLDAWAY, 1972; LIOU, 1973) involve epidote solid solutions and thus yield less readily interpretable constraints on the solution properties of grandite. For that reason, data from these latter two studies are not analyzed in the present paper.

2.2. THEORETICAL WORK

HOLDAWAY (1972) and PERCHUK and ARANOVICH (1979) interpreted their experimental data to indicate, within the analytical uncertainties, ideal solution behaviour for the grossular and andradite components. It was concluded that component activities in the binary system are adequately expressed by a two-site model:

$$a_{gro} = (X(Ca_3Al_2Si_3O_{12}))^2 \quad (1)$$

and

$$a_{and} = (X(Ca_3Fe_2Si_3O_{12}))^2 \quad (2)$$

BIRD and HELGESON (1980, 1981) also advocated this type of an ideal ionic model on the basis of general crystal chemical arguments, especially the assumed randomness in the Al-Fe^{3+} distribution over the two sites. However, recent crystallographic studies indicate that substantial ordering between these sites (M1 and M2) does occur and may be responsible for an ultimate reduction in symmetry (TAKEUCHI and HAGA, 1976; MARIKO and NAGAI, 1980; TAKEUCHI et al., 1982; HIRAI and NAKAZAWA, 1986), as observed in several X-ray studies and commonly evidenced by optical anisotropy of calcic garnet in thin section. These new crystal-chemical data render doubtful whether the ideal solution model proposed earlier is adequate, at least at low temperatures and for grossular-rich compositions. Indeed, positive deviations from ideality have been proposed by WASSERMANN et al. (1982) for the grossular component, although they performed their analysis based on an ideal molecular model, i.e. assuming

$$a_{gro} = X(Ca_3Al_2Si_3O_{12}) \cdot \gamma(Ca_3Al_2Si_3O_{12}) \quad (3)$$

Such a formulation is inadequate on statistical-mechanical grounds (COHEN, 1986). For this reason and because the results of WASSERMANN et al.'s data analysis are not given in analytical form, their excess terms are not readily comparable with those of the ionic model derived below.

We present below the results of a careful analysis of all of the experimental data, notably including those of HOLDAWAY (1972) and HUCKENHOLZ et al. (1981). Mathematical programming methods (BERMAN et al., 1986) were applied to investigate the internal consistency of the data and to derive empirical activity-composition relations. We confirm that the grandite solution behaviour is strongly asymmetric, showing negative departure from ideality for Fe-rich compositions and a positive excess free energy in the Al-rich part of the composition range. The model so derived is at least qualitatively compatible with the observed ordering of calcic garnet and the apparent compound formation at low temperatures.

Apparent inconsistencies with previous models are due to unwarrented simplifying assumptions made in the literature about the solution behaviour of phases coexisting with grandite, such as aqueous chloride fluids (PERCHUK and ARANOVICH, 1979) or the epidote solid solution (BIRD and HELGESON, 1980, 1981).

3. Mixing properties of the grandite solution

3.1. MOLAR VOLUME DATA

Table 1 contains a compilation of reliable X-ray unit cell measurements of grandites, most of them synthetic. By contrast to the volume data of pure grossular which indicate only minor scatter ($125.270 \pm 0.007\ cm^3mol^{-1}$), the cell dimensions reported for endmember andradite depend on synthesis conditions (GUSTAFSON, 1974). Even disregarding samples prepared hydrothermally at low temperature which probably contain some hydroandradite component ($Ca_3Fe_2(OH)_{12}$), the weighted average of the molar volume data for andradite ($131.937 \pm 0.013\ cm^3mol^{-1}$) show more variability than those for grossular.

Among the data for intermediate calcic garnets, only those of HUCKENHOLZ et al. (1981) for synthetic grandite and of MEAGHER (1975) for a natural near-binary garnet yield a uniform pattern. A very minor negative excess volume of mixing is indicated by these data (Fig. 2). By contrast, the synthetic samples prepared by LIOU (1973), as well as natural calcic garnets reported by BABUSKA et al. (1978) show somewhat larger unit cells, but also much greater scatter. Within their uncertainty, LIOU's data follow Vegard's Law, i.e. they require no excess volume. The reasons for the discrepancy with the data of HUCKENHOLZ et al. are not known. However, a very small amount of hydrogarnet component cannot be ruled out and would suffice to explain the observed cell increase in LIOU's samples.

Inasmuch as the cell dimensions reported by HUCKENHOLZ et al. (1981) are the smallest and their variation with composition the most regular, an expression for the excess volume of mixing for grandite was derived from these data only. Weighted least squares regression to an asymmetric Margules model

$$V_{xs} = X_{gro}X_{and}(W_{V,gro}X_{gro} + W_{V,and}X_{and}) \quad (4)$$

Tab. 1 Cell parameter and molar volume data of anhydrous grandite.
Bracketed numbers indicate uncertainly in the digits to their immediate left.

Source	X_{gro}	X_{and}	X_{alm}	X_{pyr}	X_{spe}	a_o [A]		V [cm^3/mol]	
Skinner 1956	1.					11.851(1)		125.31(3)	
Pistorius & Kennedy 1960	1.					11.850		125.26	
Newton 1965	1.					11.850		125.26	
Robie et al 1967	1.							125.30(3)	
Liou 1973	1.					11.852(2)		125.32(7)	
Huckenholz et al 1975	1.					11.845(3)		125.10(10)	
Huckenholz et al 1975	1.					11.850		125.26	
Newton et al 1977	1.					11.849(1)		125.23(2)	
Charlu et al 1978	1.					11.849(1)		125.23(2)	
Cressey et al 1978	1.					11.849(1)		125.23(3)	
Hazen & Finger 1978	1.					11.846(1)	L	125.13(3)	
Shmulovich 1978	1.						H	125.48	
Kolesnik et al 1979	1.						H	125.55(9)	
Krupka et al 1979	1.							125.26(4)	
Krupka et al 1979	1.							125.35(4)	
Perchuk & Aranovich 1979	1.					11.827(7)		124.52(22)	
Perchuk & Aranovich 1979	1.					11.851(2)		125.30(5)	nat
Haselton & Westrum 1980	1.							125.28(1)	
Hsu 1980	1.					11.849(2)		125.23(5)	
* Weighted average	1.							125.270(7)	
Meagher 1975	.962	.025			.013	11.846(2)		125.13(7)	nat
Huckenholz et al 1974	.900	.100				11.866(2)		125.77(7)	
Holdaway 1966	.842	.126	.003	.029		11.877(3)		126.12(10)	nat
Huckenholz et al 1974	.800	.200				11.882(2)		126.28(7)	
Babuska et al 1978	.799	.142	.032	.022	.004	11.870(2)		125.90(7)	nat
Babuska et al 1978	.761	.221		.005	.013	11.910(5)		127.17(16)	nat
Liou 1973	.750	.250				11.904(2)		126.98(7)	
Huckenholz et al 1974	.700	.300				11.896(4)		126.72(13)	
Huckenholz et al 1974	.600	.400				11.920(3)		127.49(10)	
Huckenholz et al 1974	.500	.500				11.943(2)		128.23(7)	
Liou 1973	.500	.500				11.956(2)		128.65(7)	
Huckenholz et al 1974	.450	.550				11.953(3)		128.55(10)	
Huckenholz et al 1974	.400	.600				11.965(3)		128.94(10)	
Huckenholz et al 1974	.300	.700				11.987(1)		129.66(3)	
Liou 1973	.250	.750				12.005(2)		130.24(7)	
Babuska et al 1978	.222	.704	.041	.028	.005	12.009(1)		130.37(3)	nat
Huckenholz et al 1974	.200	.800				12.011(3)		130.44(10)	
Huckenholz et al 1974	.100	.900				12.032(3)		131.12(10)	
Skinner 1956		1.				12.048(1)		131.69(3)	
Swanson et al 1960		1.				12.059			
Naka et al 1968		1.				12.062			
Huckenholz & Yoder 1971		1.				12.054(2)		131.84(7)	
Huckenholz & Yoder 1971		1.				12.056(3)		131.91(10)	
Huckenholz & Yoder 1971		1.				12.059(3)		132.01(10)	
Liou 1973		1.				12.055(2)		131.87(7)	
Gustafson 1974		1.				12.0560(5)		131.91(2)	
Gustafson 1974		1.				12.0580(5)		131.97(2)	
Liou 1974		1.				12.064(4)		132.17(13)	
Suwa et al 1976		1.				12.059(3)		132.01(10)	
Suwa et al 1976		1.				12.051(3)		131.74(10)	
Taylor & Liou 1978		1.				12.061(3)		132.07(10)	
Perchuk & Aranovich 1979		1.				12.056(7)		131.91(22)	
Perchuk & Aranovich 1979		1.				12.048(2)		131.65(5)	nat
* Weighted average		1.						131.937(13)	

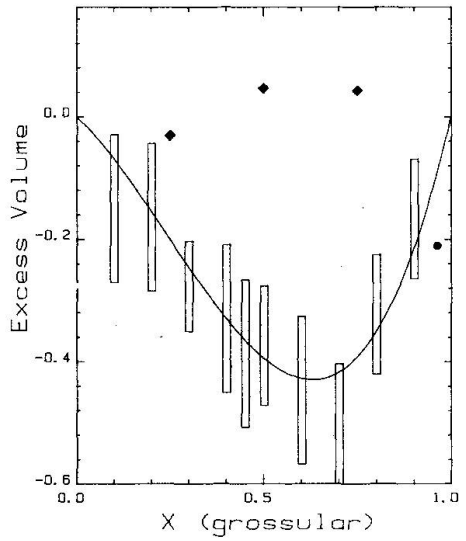

Fig. 2 Excess molar volume (cm^3mol^{-1}) of mixing for binary grossular-andradite samples. Data with error bars from HUCKENHOLZ et al. (1981) were used for least squares fit (solid curve, equation 4). Filled symbols refer to data not included in the fit (diamonds: LIOU, 1973; circle: MEAGHER, 1975).

Tab. 2 Experimental data on equilibrium (5).

X_{gro}	Temp (°C)	P_x (bar)	P_1	Polymorphs	Ref
0.940	772	6000	6214	qz,wo	1
0.734	700	4000	4613	qz,wo	1
0.601	625	2000	2988	qz,wo	1
0.592	750	4000	5721	qz,wo	1
0.523	790	4000	6622	qz,wo	1
0.514	680	2000	4170	qz,wo	2
0.465	740	2068	5500	qz,wo	1
0.455	750	2000	5721	qz,wo	1
0.419	840	2000	7759	qz,wo	1
0.388	750	1	5239	tr,pswo	1
0.352	850	1	8021	tr,pswo	1
0.310	950	1	10877	tr,pswo	1
0.255	1050	1	13804	tr,pswo	1
0.241	1110	1	15596	tr,pswo	1

Ref. 1: HUCKENHOLZ et al. (1981)
2: HOLDAWAY (1972), his value of X_{gro} was adjusted to correct for different cell parameters used.

yields

$$W_{V,gro} = -2.60\ cm^3mol^{-1}$$
$$W_{V,and} = -0.55\ cm^3mol^{-1}$$

The excess volume (Fig. 2) shows only slight asymmetry in X_{gro} but, by contrast to the model implied by Figures 1 and 3 of WASSERMANN et al. (1982), V_{xs} is negative throughout. The discrepancy to their model seems to be primarily due to the volume data for pure grossular.

3.2. ACTIVITY-COMPOSITION RELATIONS

Only two of the experimental data sets involving grandite equilibria (HOLDAWAY, 1972; HUCKENHOLZ et al., 1981) yield activity values for a grandite component without requiring any assumption on the solution behaviour of another Al-Fe^{3+}-phase. Both studies consider the displacement by Fe^{3+} of the equilibrium

$$\underset{\text{garnet}}{Ca_3Al_2Si_3O_{12}} + \underset{\text{quartz or tridymite}}{SiO_2} = \underset{\text{anorthite}}{CaAl_2Si_2O_8} + \underset{\text{wollastonite or pseudowollastonite}}{2\,CaSiO_3} \qquad (5)$$

and, together, they span a wide range in temperature, pressure and grandite composition (Tab. 2). In each experiment the four-phase assemblage was equilibrated at fixed P, T and bulk composition, with run durations of 10 days ($T > 1100$ °C) to 6 weeks ($T < 750$ °C). Garnet composition was measured by powder X-ray diffraction of the products. In most cases, the reported experimental details do not indicate the sense of the reaction, except in one reversal by HOLDAWAY (1972). Nonetheless, complete equilibration is likely for the data of HUCKENHOLZ et al. (1981, Table 2) as well, because they report average grandite compositions from 2–5 experiments (at any given P and T), each starting from different (but unspecified) X_{gro}.

Assuming, therefore, that the data in Table 2 do represent equilibrium (5), activity-composition relations for grandite can be obtained as shown schematically in Figure 3. Neglecting the minor Fe-contents of anorthite and wollastonite and adopting the usual standard state of unit activity for the pure components at any P and T, the equilibrium condition demands that

$$RT\ln(a_{gro}) = \int_{P_x}^{P_1} \Delta_5 V\, dP \qquad (6)$$

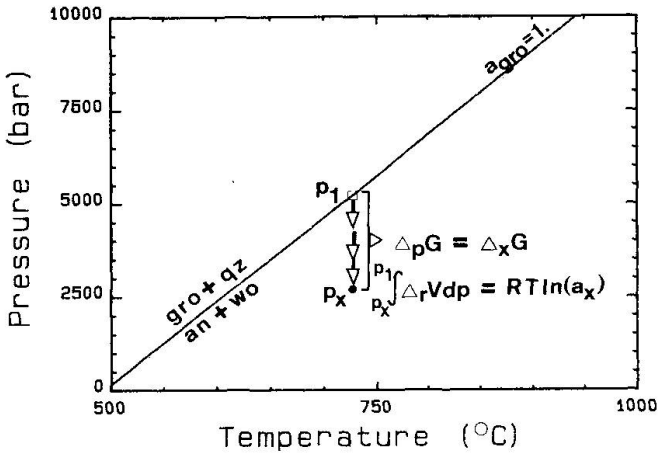

Fig. 3 The isothermal shift from P_1 to P_X in equilibrium (5) is compensated by a reduction in the activity of grossular.

where the integral is taken from P_x, the equilibrium pressure at reduced grossular activity (where $x = X_{gro}$) up to P_1, the equilibrium pressure for pure grossular, all at temperature T, and R is the universal gas constant. Expanding the volume terms as

$$V(P,T) = V_o + A_1(T-T_o) + A_2(T-T_o)^2 + B_1(P-P_o) + B_2(P-P_o)^2 \quad (7)$$

and combining (6) with (1) yields an expression for the activity coefficient of grossular for a given T, P_x, and X_{gro} (Fig. 3):

$$2\,R\,T\ln(\gamma_{gro}) = (P_1-P_x)(V_o + A_1(T-T_o) + A_2(T-T_o)^2 + P_x(B_1-B_2P_o)) + (P_1^2-P_x^2)(B_1-2B_2P_x)/2 + (P_1^3-P_x^3)B_2/3 \quad (8)$$

The accuracy of activity coefficients so derived depends crucially on our knowledge of $P_1(T)$, the equilibrium condition for (5) in the Fe-free system. While it is possible to calculate $P_1(T)$ from available calorimetric data (WASSERMANN et al., 1982) or to rely on the several sets of direct experimental brackets for equilibrium (5), these methods bear an unnecessary risk of introducing systematic errors. By contrast, our approach (BERMAN et al., 1986) considers all of the available calorimetric and phase equilibrium data simultaneously in deriving a consistent and optimized thermodynamic data base for all of the phase components involved.

We used the nonlinear mathematical programming methods described by BERMAN et al. to obtain the standard state properties (Table 3) which then yielded the $P_1(T)$ values in Table 2. The combined uncertainties in T, $P_1(T)$, P_x and X_{gro} were propagated into $\sigma R\,T\ln(\gamma_{\gamma_{gO}})$ which was adopted as an approximate standard deviation in subsequent computations. Errors in the standard state volumes and in V(P,T) of the minerals are small owing to the optimization methods used in the derivation. Therefore, possible systematic errors of this kind were ignored.

Figure 4 depicts the results of the first step of data analysis. Application of (8) and the error propagation outlined above yield the data shown by error bars. In the discussion that follows, we shall refer to these data as the "VdP-data". It is instructive to compare these to values shown as solid symbols (Fig. 4) which indicate nominal results (uncertainties not shown) of an identical analysis, but in which the common approximation (e.g. HOLLAND, 1983)

$$\int_{P_x}^{P_1} \Delta_r V\,dP = \Delta_r V(P_1-P_x) \quad (9)$$

was made. The data symbolized by diamonds

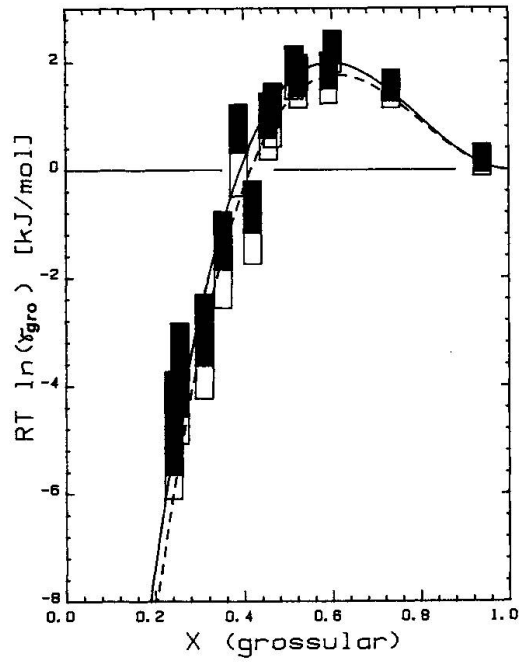

Fig. 4 The excess free energy (per mole of $Al+Fe^{3+}$) as a function of grandite composition. Symbols explained in text. Solid curve from equation (8); dashed curve assumes approximation (9).

Tab. 3 Standard state thermodynamic properties of phases considered.

ST is the code for standard state properties - G, H, S, V. Molal units: J, J, J/K, J/bar.

C1 is the code for the first line of Cp terms - K0, K1, K2, K3. Molal units: Cp in J/K.

T1 (T3, T5) is the code for the first line of transition terms. For each transition the following is needed: T_{trans} (K); reference T for integration; lambda Cp terms L_1 and L_2 (BERMAN and BROWN, 1985); heat of transition. Molal units: J and K.

T2 (T4, T6) is the code for the second line of transition terms. For each transition the following is needed: dT/dP slope of transition, parameter for higher order fit of transition T as function of P, dV/dT for low T polymorph, dV/dP for low T polymorph. Molal units: J, bar, K.

V1 is the code for the terms describing volume as a function of P, T (eq. 7).

Heat capacity equation (BERMAN and BROWN, 1985) is: $Cp = K_{0 + K1T^{-0,5} + K_{2T^{-2}} + K_{3T^{-3}}} \ldots\ldots$

ANORTHITE		$CA_1AL_2SI_2O_8$		An	
ST		-4230207.50	199.4396	10.075	
C1	439.36938	-3734.149	0.0	-317023232.	
V1	1.04113548	0.00030471	-0.14020248	0.00070471	
CALCITE		$CA_1C_1O_3$		Cc	
ST		-1206970.80	91.7929	3.690	
C1	178.18748	-1657.697	-482722.000	166604928.	
V1	0.91738718	0.00224963	-0.21141076	0.00027104	
GROSSULAR		$CA_3AL_2SI_3O_{12}$		Gr	
ST		-6633577.40	255.4265	12.536	
C1	573.43042	-2039.405	-18887168.000	2319311872.	
V1	1.81167898	0.00080806	-0.07315774	0.00031030	
A-QUARTZ		SI_1O_2		aQz	
ST		-910699.90	41.4600	2.269	
C1	80.01199	-240.276	-3546684.000	491568384.	
V1	2.38945698	0.0	-0.24339298	0.00101375	
T1	848.00	373.00	-0.09186959	0.00024607	0.0
T2	0.023743	0.0	0.0	0.0	
B-QUARTZ		SI_1O_2		bQz	
ST		-908626.73	44.2068	2.370	
C1	80.01199	-240.276	-3546684.000	491568384.	
V1	0.0	0.0	-0.12382672	0.00070871	
LOW TRIDYMITE		SI_1O_2		lTr	
ST		-907616.64	44.1568	2.699	
C1	75.37267	0.0	-5958095.	958246144.	
V1	1.93394983	0.0	-0.25084238	0.0	
T1	390.15	298.15	0.42670490	-0.00144575	130.54
HIGH TRIDYMITE		SI_1O_2		hTr	
ST		-907100.19	45.4753	2.732	
C1	75.37267	0.0	-5958095.	958246144.	
V1	0.48286524	0.0	-0.07396833	0.00037354	
WOLLASTONITE		$CA_1SI_1O_3$		Wo	
ST		-1631545.20	81.7700	3.983	
C1	149.07266	-690.295	-3659348.000	484349440.	
V1	1.97553101	-0.00037158	-0.13781321	0.00069295	
PSEUDOWOLLASTONITE		$CA_1SI_1O_3$		Pwo	
ST		-1627258.22	85.3994	4.022	
C1	141.15611	-417.232	-5857595.000	940734976.	
V1	1.97553101	-0.00037158	-0.13781321	0.00069295	

and the corresponding model will be termed "PV-approximation" below. Figure 4 would suggest that the difference between the VdP-data and the PV-approximation is minor, except that the excess free energy implied by the latter is systematically lower (more negative). Some consequences of this discrepancy will be explored below.

Figure 4 emphasizes the asymmetry in X_{gro} of the grandite solution model. However, the strong (negative) correlation between T and X_{gro}—experiments at higher temperatures generally yielded grandite with lower X_{gro}—afford no clean separation of a possible T-dependence in the excess free energy. Because the compositional dependence is likely to outweigh the effect of temperature and because attempts to include excess entropy terms in the fit resulted in unrealistic values, a subregular solution model was deemed adequate. We thus fit the data (Table 2) to

$$2\,R\,T\ln(\gamma_{gro}) - X_{gro}X_{and}(X_{gro}W_{G,gro} + X_{and}W_{G,and}) = 0 \qquad (11)$$

by means of least squares regression, using the inverse estimated variance ($\sigma^{-2}_{RT\ln(\gamma_{gro})}$) as a weighting factor. For the VdP-data the resulting Margules parameters are

$$W_{G,gro} = +12.906\ kJ\,mol^{-1}$$
$$W_{G,and} = -46.910\ kJ\,mol^{-1}$$

which yield the solid curve in Figure 4. As expected, the representation of the data is satisfactory, as it is also for the model shown by the dashed line that results from a fit to the PV-approximation data. Comparison with Figure 5 of WASSERMANN et al. (1982) shows that, as a consequence of the inadequate activity model (3) they chose, their excess free energy is quite temperature-dependent, whereas it is T-invariant in the present model (11).

Activity-composition relations computed from the VdP model using

$$a_{gro} = X^2_{Al}\exp\left(X^2_{Fe}(W_{gro} + 2X_{Al}(W_{and}-W_{gro}))/(RT)\right) \qquad (12a)$$

and

$$a_{and} = X^2_{Fe}\exp\left(X^2_{Al}(W_{and} + 2X_{Fe}(W_{gro}-W_{and}))/(RT)\right) \qquad (12b)$$

are shown in Figure 5. The deviation from ideal (ionic) is evidently positive for the grossular component, at least for Fe-poor grandites. By contrast, the andradite component shows an even stronger negative deviation over most of the composition range. For grossular-rich grandites, the positive excess free energy dominates the configurational contribution at temperatures below 444 °C, predicting a distinctly asymmetric solvus (Fig. 6). Iso-activity lines, shown here for the grossular component only, are quite temperature-dependent at high grossular contents.

It is in the activity-composition diagram that some remarkable differences emerge between the VdP-model and the PV-approximation. Figure 7 shows two isotherms of a_{gro} computed from each model. Except for Fe-poor compositions, the PV-approximation (dashed curves) yields somewhat lower values of a_{gro} even at high temperatures (1000 °C). The discrepancy becomes considerable at temperatures below 500 °C such that, for example, at the critical temperature for unmixing predicted by the PV-approximation model (322 °C), the VdP-model predicts a miscibility gap for compositions $0.66 < X_{gro} < 0.94$. Solution models derived from high pressure phase equilibrium data generally appear to be more sensitive to

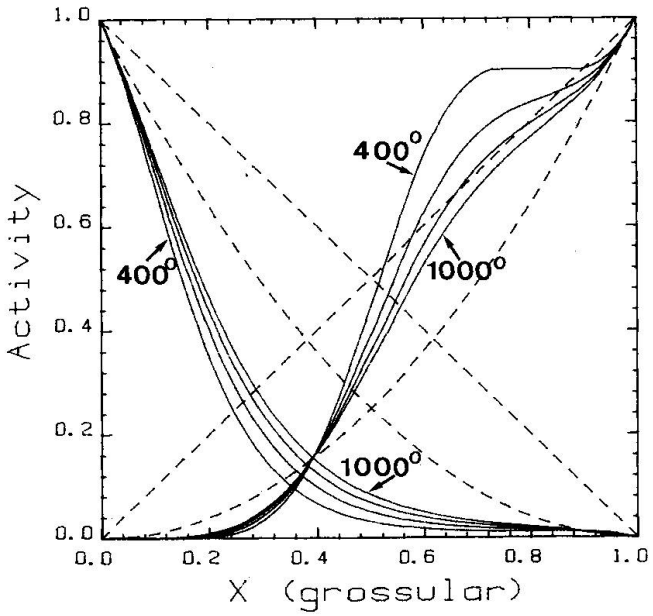

Fig. 5 Computed isotherms (at 200° intervals) in activity-composition space. For comparison: Dashed curves = ideal ionic models (1) and (2). Diagonals = ideal molecular models ($a_i = X_i$).

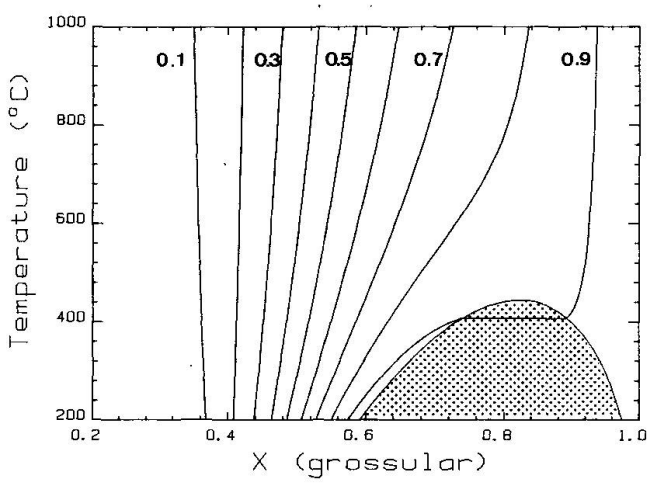

Fig. 6 Computed lines of constant grossular activity and two-phase region (stippled) of grandite at low temperature (P = 1 bar).

the assumed V(P,T) behaviour than was hitherto recognized. This conclusion rests on several solutions in addition to the grandite example and underscores the need for accurate volume data for minerals at high P and T.

In summary, the available phase equilibrium data indicate that grandite behaves as a strongly asymmetric, approximately subregular solution. The excess enthalpy is quite negative for Fe-rich members, whereas it is moderately positive for Fe-poor grandites. A solvus is predicted with a critical temperature of 444 °C (at $X_{gro} = 0.82$). The extent of the two-phase region and the details of the activity-composition relations are surprisingly sensitive to errors introduced by the assumption that the volume of reaction is independent of P and T (approximation 9).

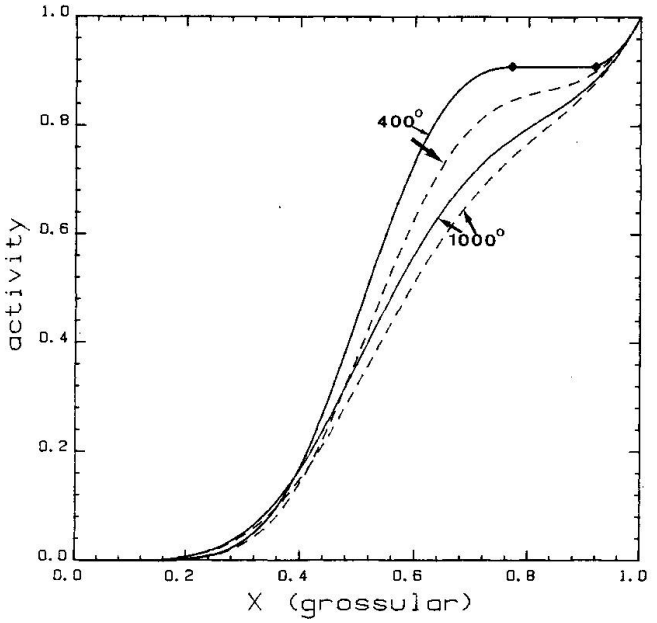

Fig. 7 Comparison of isotherms in a_{gro} according to VdP model (solid curve) and PV-approximation (dashed).

4. Crystal chemical causes of the nonideal solution behaviour

Considering the known complexities (such as optical anisotropy, cation ordering, phase separation) in some grandite-rich garnets, the thermodynamic model developed above certainly has its limits in describing the real solution behaviour even approximately. The functional form of a subregular model was chosen merely for convenience and offers little insight into the details or crystal chemical reasons of the particular behaviour of grandite. A full analysis of the data on ordered and exsolved or non-cubic calcic garnets is beyond the scope of the present paper, but a few general conclusions are justified.

The magnitude of the positive deviation from ideality observed in part of the system is in accord with the systematics compiled by DAVIES and NAVROTSKY (1983) which established a general correlation between volume mismatch and excess free energy parameter. Because these systematics derive primarily from solutions in which singly or doubly charged ions are mixed, the present case involving Al^{3+} and Fe^{3+} is expected to yield a somewhat more positive interaction parameter than the correlation predicts (NAVROTSKY, 1982). Indeed, we obtained $W_{G,gro} = +12.9$ kJ mol^{-1}, whereas DAVIES and NAVROTSKY (1983) would predict only 4.8 kJ mol^{-1}. It is noteworthy, however, that for solutions as strongly asymmetric as the one considered here, any correlation based on interaction parameters is less satisfactory than a comparison of the actual excess free energy (or enthalpy). In our sample, the two interaction parameters clearly counteract each other; in the absence of a strongly negative $W_{G,and}$ the required positive deviation for Al-rich grandite would be well described by $W_{G,gro} = 5$ to 7 kJ mol^{-1}. Nonetheless, it seems possible to connect the observed positive excess free energy for gro-

rich grandite with strain effects induced by Fe^{3+} substituting for the smaller Al^{3+}. This interpretation is also in line with the asymmetry in the solution behaviour, because it appears to be generally "easier" to substitute a smaller component into a lattice of larger unit cell than vice versa.

However, these consideration in no way account for the pronounced negative excess free energy found over much of the compositional range. In general terms, such behaviour is indicative of order, presumably involving Al- and Fe^{3+}-ions on the octahedral sites. Based on recent crystallographic data, which appear consistent with a convergent disordering process, a simple BRAGG-WILLIAMS model of cooperative Al–Fe disordering has been tested. For realistically low temperatures of critical disordering, say $T_c < 1000\,°C$, the predicted energy of ordering turns out to be of the correct order of magnitude to account for the observed negative excess free energy of mixing. It must be emphasized again, that comparison on the basis of the interaction parameters alone is misleading owing to the pronounced asymmetry. The positive value in $W_{G,gro}$ "fights" the strongly negative term which dominates at intermediate and Fe-rich compositions. The fact that structural investigations of isotropic (high-temperature) grandite generally failed to detect considerable short range order amongst the trivalent cations, need not be in conflict with our ordering model, for the equilibrium degree of ordering at temperatures $T < (2/3)T_c$ is small over a large range of composition (see e.g. NAVROTSKY and LOUCKS, 1982) and is thus difficult to verify by structure refinement, except at compositions near $X_{gro}/X_{and} = 1$.

A close connection must exist between the solution behaviour and the microstructural mechanism, especially cation ordering and possibly cluster formation, leading ultimately to chemically inhomogeneous domains. Recent work summarized by TAKEUCHI (1986) emphasizes the structural complexities involved, however, and no simple model is likely to be able to connect the known structural and thermodynamic data. It appears, for instance, that in chemically distinct lamellae one phase is typically anisotropic, whereas directly adjacent lamellae are (optically) isotropic. Ordering apparently can lead to a reduction in symmetry for some intermediate grandites, complicating further their energetics and rendering inadequate the present simple solution model, at least for such samples. Indeed, even for isotropic parts of (presumably coherent) intergrowth, our model is at best an approximation and the miscibility gap predicted above for (cubic) grandite cannot be expected to pertain.

Summarizing, further work is needed to establish a quantitative link between the structural properties of grandite and its thermodynamic properties, especially the negative portion of its excess free energy. We conclude here that $Al–Fe^{3+}$ ordering is likely to be responsible, whereas strain effects in grossular-rich members of the series may account for the positive deviation.

5. Petrological applications of the grandite model

The solution model derived in the preceding chapter permits analysis of a number of critical mineral equilibria, especially in siliceous calcic marbles and calc silicate rocks, including skarns. Assemblages involving grossular-rich garnet are widespread and critical phase relations, including the stability of grossular itself, have been identified by field work (e.g. MISCH, 1964; TROMMSDORFF, 1968 and 1972) as well as the laboratory studies cited above. Towards high temperature, the stability limits for grandite in SiO_2-undersaturated systems, are defined by

$$\text{grossular} = \text{anorthite} + \text{wollastonite} + \text{gehlenite} \quad (13)$$

and

$$\text{grossular} + \text{corundum} = \text{anorthite} + \text{gehlenite} \quad (14)$$

whereas

$$\text{grossular} + \text{quartz} = \text{anorthite} + \text{wollastonite} \quad (5)$$

limits the upper thermal stability for quartz-saturated compositions. All of these critical equilibria are obviously affected by solid solution effects in grandite and the present activity model can be usefully applied.

At low temperature, mixed-volatile (CO_2–H_2O) equilibria are of particular petrological interest because grossular is confined to a field relatively low in X_{CO_2} (GORDON and GREENWOOD, 1971). Phase diagrams (Fig. 8) depicting these stability relations were computed based on the thermodynamic data in

Table 3 for the phases considered above and additional data consistent with that table (updated from BERMAN et al., 1985). Two main petrological applications derive from these and subsequent equilibrium calculations: a geothermometer and a series of useful T-X(CO_2) constraints.

5.1. GEOTHERMOMETRY

Inspection of figure (8) shows that for known activity of grossular (and anorthite), the equilibrium temperature may be determined for any pressure. An approximate analytical solution of the equilibrium condition of (5) is given by

$$T_{eq} = [\Delta_r V°(P_{eq} + \Delta_r H°) - (1-X_{gro})^2(W_{and} + 2X_{gro}(W_{gro} - W_{and}))]/[\Delta_r V°\Delta S° + R(2\ln(X_{gro}) - \ln(a_{an}))] \quad (15)$$

which, for pressures below 5 (10) kbar, yields results within 7° (18°) of the complete equilibrium calculation. The latter can easily be obtained by iterative refinement of $\Delta_0 V$ as a function of P_{eq} and T_{eq}.

The accuracy of this thermometer (15) is limited primarily by uncertainties in the activity models of grandite and plagioclase, in the mineral analyses, as well as in pressure. Clearly, the thermometer can be no better than the underlying data. Application to the experimental data in Table 2 yields the following residual temperatures:

Maximum deviation overall	21°
Average deviation overall	9°
Maximum deviation for T < 800 °C	16°
Average deviation for T < 800 °C	7°

For garnet close to the grandite binary, typical uncertainties from microprobe analyses add a systematic error of between 2° and 8° to T_{eq}, to which a potentially considerable uncertainty must be added if garnet is substantially non-binary, e.g. due to hydrogarnet- or Ti-components, and if the plagioclase is very sodic, such that the available solution models are questionable.

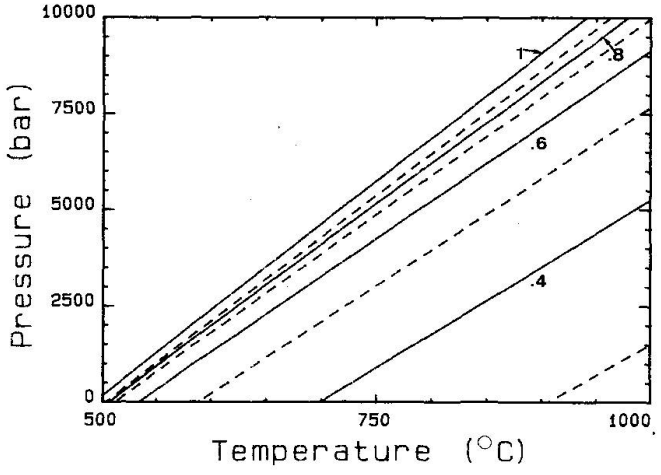

Fig. 8 Calculated isopleths of grossular activity for grandite in equilibrium with anorthite, quartz (tridymite), and wollastonite.

6. Calc-silicate assemblages in contact aureoles

Calc-silicate and skarn samples collected in the vicinity of the Adamello and the Bregaglia granitoid intrusives (Fig. 9) commonly contain low-variance assemblages, including notably calcic garnet (gar) + quartz (qz) + plagioclase (plag) + wollastonite (wo) and/or calcite (cc), though frequently one or two of these phases are missing. Instead of them or in addition, silicates such as diopside (dio), K-feldspar (Ksp), scapolite (scap), or idocrase (ido) typically occur. Phase relations involving the latter three are not reported here, because we intend to focus on some common equilibria near the chemical subsystem CaO-Al_2O_3-Fe_2O_3-SiO_2-(CO_2-H_2O). Thus, we selected samples for further analysis which contain at least two "simple" calc-silicate phases in addition to garnet and which satisfied our criteria of textural equilibrium. Short descriptions of these samples and references to their geological context are given in Appendix 1. Electron microprobe analyses obtained for garnet (Tab. 4, Fig. 1) and plagioclase indicate that these are nearly binary solutions; cc, wo and qz contain negligible impurities in these assemblages. Where the four phases gar, plag, wo and qz coexist, our thermometer (15) may thus be directly applied,

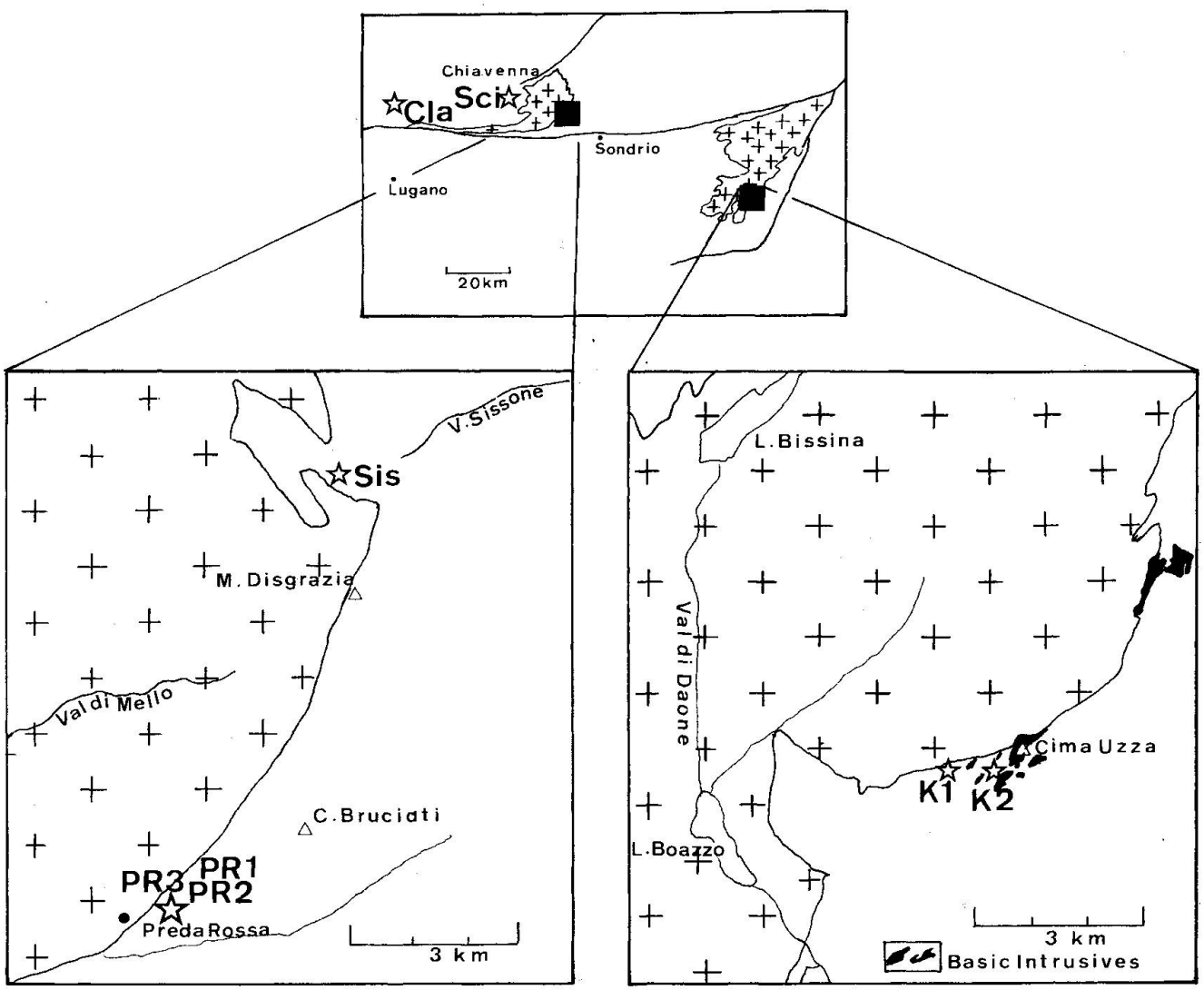

Fig. 9 Sketch map of the late alpine intrusives Bergell and Adamello (top), the eastern Bergell area (left), and the eastern Adamello (right). Stars mark sample localities. Their coordinates are given in Appendix 1.

once a solution model for plagioclase is adopted (GHIORSO, 1984). Where calcite coexists, the composition of the (CO_2–H_2O) fluid phase is fixed as well. Where one of the three phases coexisting with garnet is absent, inequality constraints on the T-X(CO_2) conditions of equilibration can be inferred.

The following sections present our results for some typical samples. First, thermometric results will be discussed and compared, where possible, to P–T-estimates obtained by other methods. Next, higher variance assemblages will be viewed in T-X(CO_2) space and, finally, examples from the recent literature on garnet-bearing calc-silicate assemblages will be reexamined in the light of the proposed solution model.

6.1. THERMOMETRY WITH GAR-PLAG-WO-QZ ASSEMBLAGES

Adamello samples

Calcic skarns occurring along the intrusive SE-contact of this body (Fig. 9) provide a useful test of our geothermometer because previous petrologic studies of these same samples yielded geothermometric results. All of the samples considered are characterized by polygonal small-scale textures.

Sample "K1" is in immediate contact with the tonalite and contains gar, qz, plag, wo and ido (Fig. 10). The critical assemblage gar–qz–plag–wo is confined to a narrow band between nearly monomineralic wollastonite and a zone

Tab. 4 Microprobe analyses of garnets from skarns around the Adamello and Bregaglia intrusives, and from Claro. For localities see Fig. 9; for associated minerals see Tables 5, 6 and Appendix 1.

	Adamello								
Sample	K1-1	K1-2	K1-3	K2-1 core	K2-1 rim	K2-2 core	K2-2 rim	K2-3 core	K2-3 rim
SiO_2	38.10	37.41	38.65	37.27	37.76	38.00	37.81	38.30	38.29
TiO_2	2.18	1.90	0.11	1.73	1.15	1.26	1.02	0.96	1.13
Al_2O_3	11.94	12.54	11.88	11.64	13.55	13.35	12.74	15.23	13.42
Fe_2O_3	12.58	12.47	15.29	13.83	12.26	12.61	12.72	9.78	11.62
FeO*	0.36	0.41	0.88	0.44	0.21	0.20	0.41	0.17	0.64
MnO	0.00	0.00	0.00	0.00	0.31	0.00	0.00	0.55	0.00
MgO	0.04	0.06	0.00	0.43	0.35	0.51	0.37	0.39	0.37
CaO	34.61	34.88	34.90	34.19	34.81	35.01	34.54	34.87	34.40
Na_2O	0.00	0.00	0.00	0.00	0.02	0.03	0.00	0.03	0.00
K_2O	0.00	0.00	0.00	0.00	0.00	0.01	0.00	0.00	0.00
Total	99.81	99.66	101.72	99.52	100.42	100.99	99.61	100.29	99.85
CATIONS assuming stoichiometry									
Si	3.026	2.969	3.020	2.972	2.958	2.961	2.993	2.977	3.014
Ti	0.130	0.114	0.007	0.104	0.068	0.074	0.061	0.056	0.067
Al	1.118	1.173	1.094	1.094	1.251	1.226	1.189	1.395	1.245
Fe^{3+}	0.752	0.745	0.899	0.830	0.723	0.739	0.758	0.572	0.688
Fe^{2+}	0.024	0.027	0.058	0.029	0.014	0.013	0.028	0.011	0.042
Mn	0.000	0.000	0.000	0.000	0.020	0.000	0.000	0.036	0.000
Mg	0.005	0.007	0.000	0.051	0.041	0.060	0.043	0.045	0.043
Ca	2.945	2.966	2.922	2.920	2.922	2.923	2.929	2.903	2.901
ENDMEMBERS									
Grossular	0.545	0.560	0.525	0.507	0.578	0.567	0.567	0.653	0.592
Andradite	0.379	0.372	0.453	0.415	0.361	0.370	0.379	0.286	0.346
Almandine	0.008	0.009	0.019	0.010	0.005	0.004	0.009	0.004	0.014
Pyrope	0.002	0.002	0.000	0.017	0.014	0.020	0.014	0.015	0.014
Spessartine	0.000	0.000	0.000	0.000	0.007	0.000	0.000	0.012	0.000
Ti-Al Gar	0.066	0.057	0.003	0.052	0.032	0.035	0.030	0.026	0.033

	Claro	Bergell							
Sample	Cla-1	Cla-3	PR1-1	PR2-1	Sis-1	Sis-2	PR3-1	PR3-2	Sci-1	Sci-2
SiO_2	38.82	38.18	38.79	38.79	39.49	39.15	38.67	38.72	38.77	39.13
TiO_2	0.00	0.00	0.00	0.00	0.00	0.66	0.00	0.51	0.57	0.00
Al_2O_3	20.90	21.05	19.72	18.68	23.09	21.78	17.87	20.58	21.38	20.65
Fe_2O_3	4.37	3.64	5.12	6.66	1.08	2.34	7.24	3.64	3.37	4.08
FeO*	0.78	4.46	0.00	0.00	0.01	0.00	0.00	0.00	0.23	0.70
MnO	0.13	0.34	0.04	0.12	0.04	0.06	0.33	0.37	0.32	0.39
MgO	0.08	0.21	0.00	0.13	0.06	0.10	0.10	0.22	0.10	0.12
CaO	36.56	32.75	37.57	37.10	37.69	37.45	36.72	36.75	36.90	36.24
Na_2O	0.00	0.00	0.00	0.00	0.00	0.00	0.00	0.00	0.00	0.00
K_2O	0.01	0.01	0.01	0.00	0.01	0.01	0.01	0.01	0.01	0.00
Total	101.64	100.66	101.24	101.48	101.47	101.55	100.94	100.80	101.66	101.32
CATIONS assuming stoichiometry										
Si	2.908	2.904	2.923	2.932	2.924	2.916	2.947	2.919	2.896	2.940
Ti	0.000	0.000	0.000	0.000	0.000	0.037	0.000	0.029	0.032	0.000
Al	1.845	1.887	1.751	1.664	2.016	1.912	1.606	1.829	1.882	1.829
Fe^{3+}	0.246	0.209	0.290	0.378	0.060	0.131	0.415	0.206	0.190	0.231
Fe^{2+}	0.049	0.284	0.000	0.000	0.000	0.000	0.000	0.000	0.014	0.044
Mn	0.008	0.022	0.003	0.008	0.002	0.004	0.021	0.024	0.020	0.025
Mg	0.009	0.024	0.000	0.015	0.006	0.012	0.012	0.025	0.011	0.013
Ca	2.934	2.669	3.033	3.004	2.990	2.988	2.998	2.968	2.953	2.918
ENDMEMBERS										
Grossular	0.855	0.786	0.856	0.805	0.967	0.911	0.784	0.867	0.874	0.857
Andradite	0.123	0.104	0.143	0.188	0.030	0.066	0.205	0.103	0.095	0.115
Almandine	0.016	0.095	0.000	0.000	0.000	0.000	0.000	0.000	0.005	0.015
Pyrope	0.003	0.008	0.000	0.005	0.002	0.004	0.004	0.008	0.004	0.004
Spessartine	0.003	0.007	0.001	0.003	0.001	0.001	0.007	0.008	0.007	0.008
Ti-Al Gar	0.000	0.000	0.000	0.000	0.000	0.018	0.000	0.014	0.016	0.000

* All iron measured as FeO

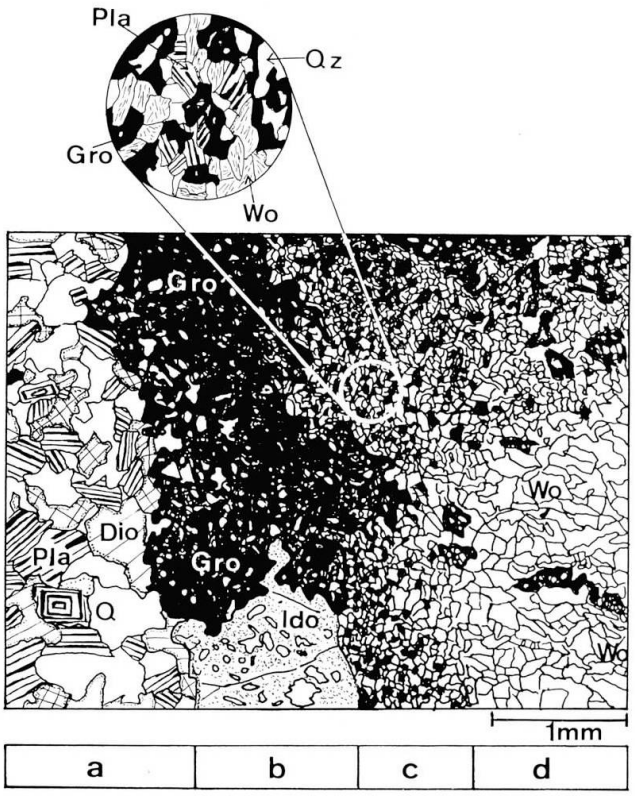

Fig. 10 Sketch from thin section of specimen K1. Fine-grained calcic skarn in contact with the Adamello intrusive. Four zones can be distinguished:
a) border tonalite (metasomatized)
b) poikiloblastic gar and ido overgrowing qz, plag and dio
c) polygonal texture of the low variance assemblage gar-plag-qz-wo
d) wollastonite zone with minor dio and gar

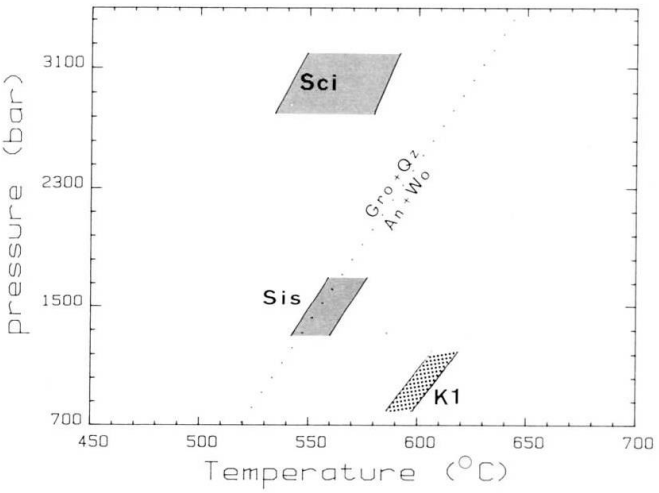

Fig. 11 P-T range of gar-qz-wo-plag equilibrium assemblages as limited by "minimum" ("maximum") isopleths, corresponding to the lowest (highest) measured values of X_{gro}/X_{an}.

containing poikiloblastic garnet and idocrase. Microprobe analyses of gar-plag pairs in this narrow band (Tab. 5) reveal nearly constant values of X_{an}/X_{gro}, for which the pertinent isopleths are calculated in a P-T-diagram (Fig. 11). Assuming a pressure of 1–1.5 kbar on the basis of tectonic and stratigraphic considerations (BRACK, 1984), we obtain a temperature range of 595–630 °C, in good agreement with data on the adjacent (overlying) dolomite (do) marbles, where calcite-dolomite thermometry yields 500–625 °C (BUCHER, 1982; VOGLER, 1985).

Bregaglia samples

A variety of calcite-rich skarns occurring at three localities (Fig. 9 and App. 1) were sampled or taken from collections at ETH Zurich. As in the Adamello samples, low variance assemblages prevail in all three localities, again

Tab. 5 Gar-plag-qz-wo assemblages: Calculated equilibrium temperatures and $X(CO_2)$. T in °C, P in kbar

sample	X_{gro}	X_{an}	X_{gro}/X_{an}	calcite	$T/P/X_{CO_2}$
K1-1	0.54	0.97	0.557	-	604 / 1 /
K1-2	0.56	0.97	0.577	-	596 / 1 /
K1-3	0.52	0.90	0.577	-	608 / 1 /
Sis-1	0.97	0.74	1.311	+	548 /1.5/ 0.10
Sis-2	0.92	0.77	1.195	+	551 /1.5/ 0.10
Sci-1	0.86	0.32	2.687	+	586 / 3 / 0.05
Sci-2rim	0.88	0.17	5.176	+	534 / 3 / 0.02
Sci-2core	0.93	0.34	2.735	-	582 / 3 /
PR-1	0.84	0.05	16.800	-	377 /1.5/

in apparent small-scale textural equilibrium. The Val Sissone sample ("Sis") displays a mosaic texture of cc-gar-wo-dio-ido-plag-qz, in which zones of bladed wollastonite typically alternate with diopside + quartz. X_{an}/X_{gro} values are again quite constant (Tab. 5). For a pressure of 1.5 kbar (TROMMSDORFF, 1966; BUCHER, 1977), an equilibration temperature near 575 °C is obtained (Fig. 11), whereas calcite-dolomite thermometry in the adjacent dolomitic marble yields temperatures of 560–600 °C.

Of the "Preda Rossa" samples, "PR1", "PR2", "PR3" were analyzed by microprobe. "PR1" is characterized by wollastonite-rich bands alternating at a mm-scale with diopside- plus quartz-rich bands in which minor garnet and sodic plagioclase occur. Here, application of (15) would indicate temperatures of only 350 °C (1.5 kbar), clearly too low for the environment of these skarns and in poor agreement with calcite-dolomite thermometry data of 520–570 °C (ENGI, 1973). However, nearby samples "PR2" and "PR3" which contain no plagioclase and for which (15) thus yields maximum temperature values, indicate about 600 °C (for $X_{an} = 1$ and P = 1 kbar), in accord with the results of calcite-dolomite thermometry. The result for "PR1" cannot be interpreted unambiguously: It may record a late reequilibration of that sample, associated with the locally observed albitization. Alternatively, the extreme dilution of the anorthite component in equilibrium (5) may push the solution model of GHIORSO (1984) beyond the range where it predicts the activity of anorthite reliably.

In the Val Schiesone sample ("Sci") a mosaic of gar-cc-qz-wo-dio-plag occurs, with poikiloblastic garnet and wollastonite and with some of the garnet forming a corona-type reaction texture around corroded scapolite. Table 5 lists compositions of the two different albite-rich plagioclase types that coexist with slightly zoned garnet. Temperatures of about 584° (3 kbar) are indicated by (15) for the plagioclase-garnet pairs with higher X_{an} (Fig. 11), in reasonable agreement with the 600 °C obtained by OTERDOOM and GUNTER (1983) for these same rocks (though employing grossular activity values that we cannot reproduce). Assuming equilibrium (5) holds for our very sodic plagioclase, (15) would indicate lower temperatures of 534 °C, perhaps indicating a slight retrograde readjustment.

6.2. T-X(CO_2) CONSTRAINTS

Various assemblages in skarns yield constraints in T-X(CO_2) space (e.g. GORDON and GREENWOOD, 1971; KERRICK, 1970 and 1977). At equilibrium, the assemblage gar-qz-plag-wo plus cc represents an isobarically invariant condition, at least in a binary CO_2-H_2O fluid. Such assemblages occur, for example in the Val Sissone and Val Schiesone samples (Tab. 5), yielding equilibrium temperatures and X(CO_2) values. For gro-bearing as-

Tab. 6 Garnet bearing assemblages with one phase absent: Calculated T-X(CO_2) constraints. T in °C, P in kbar

Sample No.	X(gro)	X(an)	absent phase	calcite	T / X(CO_2) / P
K2-1core	0.51	0.90	wo	+	<615 / >0.64 / 1
K2-1rim	0.59				<575 / >0.35 / 1
K2-2core	0.57	0.89	wo	-	<582 / >0.38 / 1
K2-2rim	0.57				<582 / >0.38 / 1
K2-3core	0.59	0.93	wo	+	<575 / >0.35 / 1
K2-3rim	0.88				<555 / >0.25 / 1
Cla-1	0.86	1.00	wo	+	<780 / >0.28 / 6
Cla-3	0.79	1.00	wo	+	>790 / >0.31 / 6
PR2-1	0.81	-	an	+	<577 / >0.17 / 1.5
PR3-1	0.78	-	an	+	<578 / >0.17 / 1.5
PR3-2	0.87	-	an	+	<575 / >0.16 / 1.5

semblages lacking one of the above minerals (Tab. 6), useful constraints on the equilibrium T-X(CO_2) conditions may still be obtained, as the following examples demonstrate.

Wollastonite assemblages

In wo-absent assemblages thermometer (15) yields maximum temperatures of equilibration. In addition, the X(CO_2) range is limited (Fig. 13a) by the coexistence of calcite and quartz, as well as by the equilibrium

$$\text{anorthite} + \text{calcite} + \text{quartz} = \text{grossular} + CO_2 \qquad (16)$$

- *Adamello samples:* K2 belongs to the same skarn unit as K1 (above), but it is considerably coarser grained and contains the assemblage gar-plag-cc-dio-qz in a mosaic fabric (Fig. 12). The composition of grandite is variable (Tab. 6), with small grains and rims of larger ones yielding a range in X_{an}/X_{gro} of 0.7–0.85. Assuming the same plagioclase was in equilibrium with the cores of these larger garnets, values of X_{an}/X_{gro} = 0.55 would be obtained, corresponding closely to sample K1. The maximum temperature of equilibration is thus about 605 °C 1 kbar and Figure 13a illustrates the X_{CO_2} range for this assemblage at equilibrium.

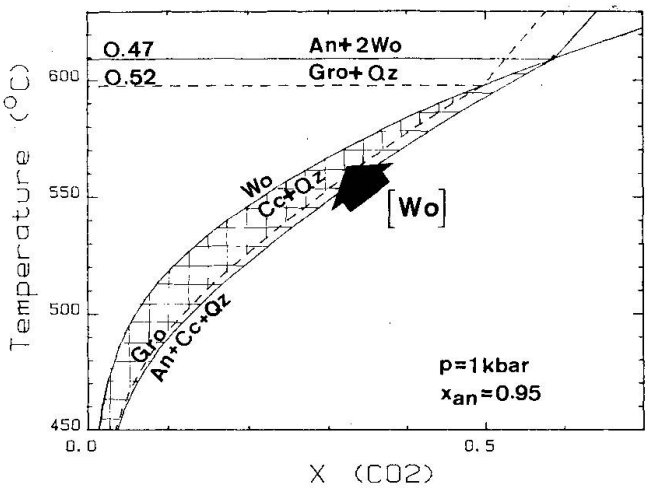

Fig. 13a T-X(CO_2) range for sample K2 with X_{gro} = 0.55. The limits are given by a_{gro} = 0.47 (X_{gro} = 0.55 at 615 °C) and by a_{gro} = 0.52 (X_{gro} = 0.55 at 400 °C).

- *Claro:* This sample derives from an amphibolite facies calc-silicate rock from the lower Pennine zone in the Ticino (TROMMSDORFF, 1968; CODONI, 1981). Massive portions of the sample contain a coarse-grained mosaic assemblage of gar-cc-plag plus idocrase and clinozoisite. Wollastonite occurs, but is restricted to veinlets and presumably formed by reaction with a channelled H_2O-rich fluid; wollastonite may thus postdate the rest of the assemblage. Maximum temperatures indicated here are below 740 °C at 5 kbar.

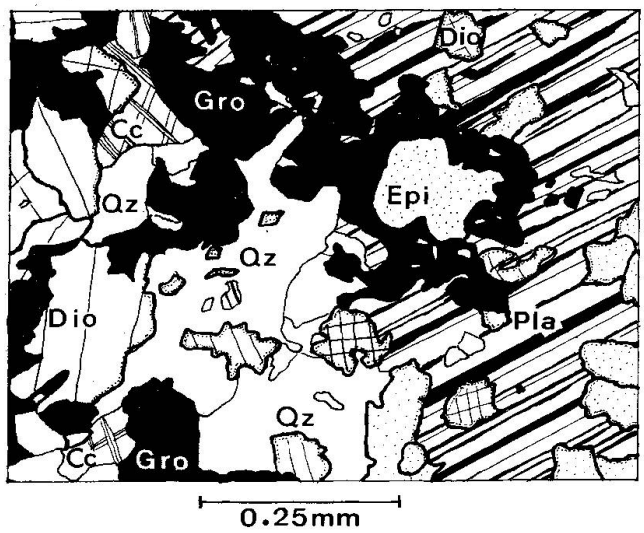

Fig. 12 Sketch from thin section of specimen K2 shows coarse-grained equilibrium assemblage, including calcite (instead of wollastonite, compare K1). Epidote (Epi) replaces garnet and plagioclase.

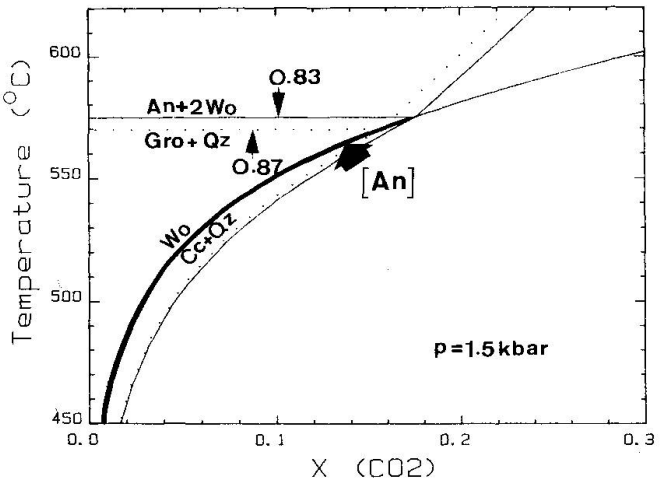

Fig. 13b T-X(CO_2) range of sample PR2 is buffered along univariant equilibrium curve cc + qz = wo + CO_2. The minimum and maximum a_{gro} values shown are calculated from X_{gro} = 0.8.

Plagioclase-absent assemblages

In plagioclase-absent assemblages application of (15) also yields maximum temperatures of equilibration. The $X(CO_2)$ range is buffered along the (isobarically) univariant equilibrium (Fig. 13b)

calcite + quartz = wollastonite + CO_2 (17)

Two of the Preda Rossa samples (PR2, PR3) lack plagioclase and contain calcite instead. The evaluated maximum equilibrium temperature corresponds to the calcite-dolomite thermometry data (above, Tab. 6), indicating that the activity of $CaAl_2Si_2O_8$ (e.g. in the fluid) was perhaps not far from unity. Fig. 13b illustrates the range of $T\text{-}X_{CO_2}$ conditions at which this assemblage could have formed, assuming equilibration in a binary CO_2-H_2O fluid.

6.3. EXAMPLES FROM THE LITERATURE

Some of the recently analyzed low-variance assemblages in the skarn literature are reexamined here, especially with regard to thermometric inferences drawn. Table 7 summarizes the $T\text{-}X(CO_2)$ conditions of various skarns as calculated by the authors and compares these with the results of our model. Keeping in mind that earlier investigators assumed grandite to behave as an ideal solution, it is expected that our equilibrium temperatures are systematically lower, at least for grossular-rich assemblages, due to the asymmetric solution behaviour of grandite. An additional though lesser difference between our findings and earlier ones stems from the different thermodynamic data employed and/or the experimental data accepted by the various studies.

Tab. 7 Comparison of evaluted equilibrium conditions from the literature and this study. Tin °C, P in kbar

Paper and Locality	Sample	Phases present	----- T (range) / P / $X(CO_2)$ ----- Literature	This Study
KERRICK (1970) Sierra Nevada, California	255	gro(90)-qz-wo	530-600 / 1-2 / <0.16	549-595 / 1.5 / <0.16
	140b	gro(50)-qz-wo-an(70)	630-670 / 1-2 / ?	612-660 / 1.5 / <0.50
KERRICK, (1977) Sierra Nevada, California	?	gro(75)-qz	<650 / 2 / <0.4	<604 / 2 / <0.18
SHEDLOCK and ESSENE (1979) Tactit (Helena), Montana	?	gro(75)-wo-an(90)	<570 / 1 / 0.12	<555 / 1 / <0.19
BOWMAN and ESSENE (1984)	?	gro(75)-qz-an(80)	<585 / 1 / 0.30?	<535 / 1 / 0.14
Elkhorn, Montana	?	gro(90)-qz-an(80)	<565 / 1 / 0.30?	<530 / 1 / 0.13
BROWN et al. (1985) Pine Creek, California	?	gro(90)-qz-wo-cc	<615 / 1.5 / <0.25	<572 / 1.5 / <0.15

7. Conclusions

The above applications of our grandite solution model to high-grade metamorphic calcsilicate assemblages underscore the consequences of the nonideal solution behaviour. Except where pervasive epithermal activity occurred, probably involving fluid infiltration, the thermometer proposed here seems to retain the high-temperature record. At present, applications in low temperature environments and in skarns containing substantially subcalcic garnets (e.g. NEWBERRY, 1983) are limited by the poorly known influence of additional components involving Ti, Mn, and H.

Acknowledgements

We are indebted to several colleagues for their help with this work. Notably, Robert G. Berman contributed results of his optimization analysis of the CASH subsystem and of the PVT behaviour of minerals. Volkmar Trommsdorff offered advice and samples from his collection. B. Ronald Frost and most especially Peter Ulmer provided helpful reviews of this paper. It is a pleasure to thank you all.

M.E. acknowledges support through the ETH Forschungsprojekt (Kredit No. 0.330.020.18/1) which covered the computing costs incurred at the University of British Columbia, Vancouver, Canada.

References

BABUSKA, V., FIALA, J., KUMAZAWA, M. and OHNO, I. (1978): Elastic properties of garnet solid-solution series. Phys. Earth Planet. Interiors, 16, 157–176.

BERMAN, R.G., ENGI, M., GREENWOOD, H.J. and BROWN, T.H. (1986): Derivation of internally consistent thermodynamic data by the technique of mathematical programming: a review with application to the system $MgO-SiO_2-H_2O$. J. Petrol., 27 (6), 1331–1364.

BERMAN, R.G. and BROWN, T.H. (1985): Heat capacity of minerals in the system $Na_2O-K_2O-CaO-MgO-FeO-Fe_2O_3-Al_2O_3-SiO_2-TiO_2-H_2O-CO_2$:representation, estimation, and high temperature extrapolation. Contr. Mineral. Petrol., 89, 168–183.

BERMAN, R.G., BROWN, T.H. and GREENWOOD, H.J. (1985): An internally consistent thermodynamic data base for minerals in the system $Na_2O-K_2O-CaO-MgO-FeO-Fe_2O_3-Al_2O_3-SiO_2-TiO_2-H_2O-CO_2$. Atomic Energy of Canada Ltd. Technical Record TR-377, 62 p. SDDO, AECL Research Company, Chalk River, Ont. KOJ 1JO.

BIRD, D.K. and HELGESON, H.C. (1980): Chemical interaction of aqueous solutions with epidote-feldspar mineral assemblages in geologic systems: I. Thermodynamic analysis of phase relations in the system $CaO-FeO-Fe_2O_3-Al_2O_3-SiO_2-H_2O-CO_2$. Am. J. Sci., 280 (9), 907–941.

BIRD, D.K. and HELGESON, H.C. (1981): Chemical interaction of aqueous solutions with epidote-feldspar mineral assemblages in geologic systems: II. Equilibrium constraints in metamorphic/geothermal processes. Am. J. Sci., 281 (5), 576–614.

BOETTCHER, A.L. (1970): The system $CaO-Al_2O_3-SiO_2-H_2O$ at high pressures and temperatures. J. Petrol., 11, 337–379.

BOWMAN, J.R. (1984): Contact skarn formation at Elkhorn, Montana. I: P-T component activity conditions of early skarn formation. Am. J. Sci., 284, 597–650.

BRACK, P. (1984): Geologie der Intrusive und Rahmengesteine des SW-Adamello (Norditalien). Diss. ETH, Zürich, 253 p.

BROWN, P.E., BOWMAN, J.R., KELLY, W.C. (1985): Petrologic and stable isotope constraints on the source and evolution of skarn-forming fluids at Pine Creek, California. Econ. Geol., 80, 72–95.

BUCHER, K. (1977): Hochmetamorphe Dolomitmarmore und zonierte metasomatische Adern im oberen Val Sissone (Provinz Sondrio, Norditalien). Diss. ETH Zürich, 249 p.

BUCHER, K. (1982): On the mechanism of contact aureole formation in dolomite country rock by the Adamello intrusion. Am. Mineral., 67, 1101–1117.

CALLEGARI, E. (1962): La cima Uzza (Adamello Sudorientale). Parte I: Studio petrografico e petrogenetico delle formazioni metamorphiche di contatto. Mem. Ist. Geol. Miner. Univ. Padova, XXIV, 1–127.

CODONI, A. (1981): Geologia e petrografia della regione di Pizzo di Claro. Diss. Univ. Zürich, 179 p.

COHEN, R.E. (1986): Statistical mechanics of coupled solid solutions in the dilute limit. Phys. Chem. Minerals, 13, 174–182.

COOMBS, D.S., KAWACHI, Y., HOUGHTON, B.F., HYDEN, G., PRINGLE, I.J. and WILLIAMS, J.G. (1977): Andradite and andradite-grossular solid solutions in very low-grade regionally metamorphosed rocks in southern New Zealand. Contrib. Mineral. Petrol., 63, 229–246.

DAVIES, P.K. and NAVROTSKY, A. (1983): Quantitative correlations of deviations from ideality in binary and pseudobinary solid solutions. J. Solid State Chem., 46, 1–22.

EINAUDI and BURT, D.M. (1982): Introduction – Terminology, classification and composition of skarn deposits. Econ. Geol., 77, 745–763.

ENGI, M. (1973): Strukturen und Metamorphose im Kontaktbereich des südwestlichen Malenco. Unpubl. Diplomarbeit ETH Zürich, 57 p.

GANGULY, J. and SAXENA, S.K. (1984): Mixing properties of aluminosilicate garnets: constraints from natural and experimental data, and applications to geothermobarometry. Am. Mineral., 69, 88–97.

GASPARIK, T. (1984): Experimental study of subsolidus phase relations and mixing properties of pyroxene in the system $CaO-Al_2O_3-SiO_2$. Geochim. Cosmochim. Acta, 48, 2537–2545.

GHIORSO, M.S. (1984): Activity/composition relations in ternary feldspars. Contr. Mineral. Petrol., 87, 282–296.

GOLDSMITH, J.R. (1980): The melting and breakdown reactions of anorthite at high pressures and temperatures. Am. Miner., 65, 272–284.

GORDON, T.M. and GREENWOOD, H.J. (1971): Stability of grossularite in H_2O–CO_2 mixtures. Am. Mineral., 56, 1674–1688.

GROBETY, B. (1985): Geologie und Petrographie am Südrand des Adamello, X. Val di Daone. Unpubl. Diplomarbeit ETH Zürich, 90 p.

GUSTAFSON, W.I. (1974): The stability of andradite, hedenbergite and related minerals in the system Ca-Fe-Si-O-H. J. Petrol., 15 (3), 455–496.

HARIYA, Y. and KENNEDY, G.C. (1968): Equilibrium study of anothite under high pressure and high temperature. Am. J. Sci., 266, 193–203.

HAYS, J.F. (1966): Lime-alumina-silica. Carnegie Inst. Wash. Year Book, 65, 234–239.

HAZEN, R.M. and FINGER, L.W. (1978): Crystal structures and compressibilities of pyrope and grossular to 60 kbar. Am. Mineral., 63, 297–303.

HIRAI, H. and NAKAZAWA, H. (1986): Grandite garnet from Nevada: confirmation of origin of iridescence by electron microscopy and interpretation of a moiré-like texture. Am. Mineral., 71, 123–126.

HIRAI, H. and NAKAZAWA, H. (1986): Visualizing low symmetry of a grandite garnet on precession photographs. Ibid., 1210–1213.

HIRAI, H., SUENO, S. and NAKAZAWA, H. (1982): A lamellar texture with chemical contrast in grandite garnet from Nevada. Am. Mineral., 67, 1242–1247.

HODGES, K.V. and SPEAR, F.S. (1982): Geothermometry, geobarometry and the Al_2SiO_5 triple point at Mt. Moosilauke, New Hampshire. Am. Mineral., 67, 1118–1135.

HOLDAWAY, M.J. (1966): Hydrothermal stability of clinozoisite + quartz. Am. J. Sci., 264, 643–667.

HOLDAWAY, M.J. (1972): Thermal stability of Al-Fe epidote as a function of f_{O_2} and Fe content. Contr. Mineral. Petrol., 37, 307–340.

HOLLAND, T.J.B. (1983): The experimental determination of activities in disordered and short-range ordered jadeitic pyroxenes. Contr. Mineral. Petrol., 82, 214–220.

HOSCHEK, G. (1974): Gehlenite stability in the system CaO-Al_2O_3-SiO_2-H_2O-CO_2. Contr. Mineral. Petrol., 47, 245–254.

HUCKENHOLZ, H.G. (1974): The grossularite relations in the CaO-Al_2O_3-SiO_2-H_2O-system: A reinvestigation up to 10 kbar. Carnegie Inst. Washington Year Book, 73, 411–426.

HUCKENHOLZ, H.G., HOELZL, E. and LINDHUBER, W. (1975): Grossularite, its solidus and liquidus relations in the CaO-Al_2O_3-SiO_2-H_2O-system up to 10 kbar. Neues Jb. Mineral., Abh., 130, 169–186.

HUCKENHOLZ, H.G. and FEHR, K.T. (1982): Stability relations of grossular + quartz + wollastonite + anorthite. II. The effect of grandite-hydrograndite solid solution. Neues Jb. Mineral., Abh., Bd. 145, 1–33.

HUCKENHOLZ, H.G., LINDHUBER, W. and FEHR, K.T. (1981): Stability relationships of grossular + quartz + wollastonite + anorthite. I. The effect of andradite and albite. Neues Jb. Mineral., Abh., Bd. 142, 223–247.

HUCKENHOLZ, H.G. and YODER, H.S. (1971): Andradite stability relations in the Ca-SiO_3-Fe_2O_3 join up to 30 kb. Neues Jb. Mineral., Abh., 114, 246–280.

KERRICK, D.M. (1970): Contact metamorphism in some areas of the Sierra Nevada, California. Geol. Soc. Am. Bull., 81, 2913–2938.

KERRICK, D.M. (1977): Genesis of zoned skarns in Sierra Nevada, California, J. Petrology, 18 (1), 144–181.

KERRICK, D.M., CRAWFORD, K.E. and RANDAZZO, A.F. (1973): Metamorphism of calcareous rocks in three pendants in the Sierra Nevada, California. J. Petrology, 14 (2), 303–325.

KERRICK, D.M. and GHENT, E.D. (1984): P-T-X_{CO_2} relations of equilibria in the system CaO-Al_2O_3-SiO_2-CO_2-H_2O. In: Problems of Physico-Chemical Petrology. Ed. by V.I. FONAREV and S.P. KORIKOVSKII, 2, 32–52. Science (Moscow).

KOLESNIK, Y.N., NOGTEVA, N.N., ARKHIPENKO, D.K., OREKHOV, B.A. and PAUKOV, I.Y. (1978): Thermodynamics of pyrope-grossular solid solutions and the specific heat of grossular at 13–300 K. Geochem. Internat., 16, 57–64.

KRUPKA, K.M., ROBIE, R.A. and HEMINGWAY, B.S. (1979): High temperature heat capacities of corundum, periclase, anorthite, $CaAl_2Si_2O_8$ glass, muscovite, pyrophyllite, $KAlSi_3O_8$ glass, grossular, and $NaAlSi_3O_8$ glass. Am. Mineral., 64, 86–101.

LIOU, J.G. (1973): Synthesis and stability relations of epidote, $Ca_2Al_2FeSi_3O_{12}(OH)$. J. Petrol., 14 (3), 381–413.

LIOU, J.G. (1974): Stability relations of andradite-quartz in the system Ca-Fe-Si-O-H. Am. Mineral., 59, 1016–1025.

MARIKO, T. and NAGAI, Y. (1980): Relations between optical properties and chemical composition of grandite. Mineral. Soc. Japan, Abstr. Ann. Meetg., C-26.

MEAGHER, E.P. (1975): The crystal structures of pyrope and grossularite at elevated temperatures. Am. Miner., 60, 218–228.

MISCH, P. (1964): Stable association wollastonite-anorthite, and other calc-silicate assemblages in amphibolite-facies crystalline schists of Nanga Parbat, Northwest Himalaya. Beitr. Mineral. Petrogr., 10, 315–356.

NAVROTSKY, A. (1982): Trends and systematics in mineral thermodynamics. Ber. Bunsenges. Phys. Chem., 86, 994–1001.

Newberry, R.J. (1983): The formation of subcalcic garnet in scheelite-bearing skarns. Can. Mineral., 21, 529–544.

NEWTON, R.C. (1966): Some calc-silicate equilibrium relations. Am. J. Sci., 264, 204–222.

NEWTON, R.C. and HASELTON, H.T. (1981): Thermodynamics of the garnet-plagioclase-Al_2SiO_5-quartz geobarometer. In: Thermodynamics of Mineral and Melts, 131–147. NEWTON, R.C. et al. (Eds.) Springer-Verlag.

OTERDOOM, W.H. and GUNTER, W.D. (1983): Activity models for plagioclase and CO_3-scapolites – an analysis of field and laboratory data. Am. J.

Sci., 283-A, 255-282.

PERKINS, D. III., ESSENE, E.J., WESTRUM, E.F. JR. and WALL, V. (1977): Application of new thermodynamic data to grossular phase relations. Contr. Mineral. Petrol., 64, 137-147.

PERCHUK, L.L. and ARANOVICH, L.YA. (1979): Thermodynamics of minerals of variable composition: Andradite-grossularite and pistacite-clinozoisite solid solutions. Phys. Chem. Minerals, 5, 1-14.

SCHMUTZ, H.U. (1976): Der Mafitit-Ultramafitit-Komplex zwischen Chiavenna und Bondasca. Beitr. geol. Karte Schweiz, Neue Folge, 149. Liefg., 73 p.

SHEDLOCK, R.J. and ESSENE, E.J. (1979): Mineralogy and petrology of a tactite near Helena, Montana. J. Petrology, 20, 1, 71-97.

SHIMAZAKI, H. (1977): Grossular-spessartine-almandine garnets from some Japanese scheelite skarns. Can. Mineral., 15, 74-80.

SHMULOVICH, K.I (1974): Phase equilibria in the system $CaO-Al_2O_3-SiO_2-CO_2$. Geochem. Internat., 11, 883-887.

SHMULOVICH, K.I. (1977): Stability limits of grossular and wollastonite in the H_2O-CO_2 system. Geochem. Internat., 14, 126-134.

SKINNER, B.J. (1956): Physical properties of end-members of the garnet group. Am. Mineral., 41, 428-436.

SOBOLEV (1964): Paragenetic types of garnets. Moscow (Publ. Acad. Sci., USSR), p. 218.

STORRE, B. (1970): Stabilitätsbedingungen Grossular-führender Paragenesen im System $CaO-Al_2O_3-SiO_2-CO_2-H_2O$. Contr. Mineral. Petrol., 29, 145-162.

SUWA, Y., TAMAI, Y. and NAKA, S. (1976): Stability of synthetic andradite at atmospheric pressure. Am. Miner., 61, 26-28.

TAKEUCHI, Y. (1986): Deviations of garnets from cubic symmetry. Abstr. Progr. Int. Mineral. Assoc., Stanford, p. 245.

TAKEUCHI, Y. and HAGA, N. (1976): Optical anomaly and structure of silicate garnets. Proc. Japan. Acad., 52, 228-231.

TAKEUCHI, Y., HAGA, N., UMIZU, S. and SATO, G. (1982): The derivative structure of silicate garnets in grandite. Zeitschr. Kristallogr., 158, 53-99.

TAYLOR, B.E. and LIOU, J.G. (1978): The low-temperature stability of andradite in C-O-H fluids. Am. Mineral., 63, 378-393.

TROMMSDORFF, V. (1966): Progressive Metamorphose kieseliger Karbonatgesteine in den Zentralalpen zwischen Bernina und Simplon. SMPM, 46, 431-460.

TROMMSDORFF, V. (1968): Mineralreaktionen mit Wollastonit und Vesuvian in einem Kalksilikatfels der alpinen Disthenzone (Claro, Tessin). SMPM, 48, 655-666.

TROMMSDORFF, V. (1972): Change in T-X during metamorphism of siliceous rocks of the Central Alps. SMPM, 52, 567-571.

VOGLER, R. (1985): Geologie und Petrographie am Südostrand des Adamello, XII. Val di Daone. Unpubl. Diplomarbeit ETH Zürich, 60 p.

WASSERMANN, A., FEHR, K.T. and HUCKENHOLZ, H.G. (1982): Partielle molare Grössen binärer Grandit-Mischkristalle. Ber. Bunsenges. Phys. Chemie, 86, 1057-1060.

WERSIN, P. (1985): Geologie und Petrographie am Südostrand des Adamello, XI. Val di Daone. Unpubl. Diplomarbeit ETH Zürich, 109 p.

WESTRUM, E.F., ESSENE, E.J. and PERKINS, D. III. (1979): Thermophysical properties of the garnet, grossular: $Ca_3Al_2Si_3O_{12}$. J. Chem. Thermodyn., 1, 543-557.

WINDOM, K.E. and BOETTCHER, A.L. (1976): The effect of reduced activity of anorthite on the reaction grossular + quartz = anorthite + wollastonite: a model for plagioclase for the earth's lower crust and upper mantle. Am. Mineral., 61, 889-896.

WOOD, B.J. (1978): Reactions involving anorthite and $CaAl_2SiO_6$ pyroxene at high pressures and temperatures. Am. J. Sci., 278, 930-942.

YODER, H.S. (1950): Stability relations of grossularite. J. Geol. 58, 221-253.

Manuscript received April 4, 1987; revised manuscript accepted June 4, 1987.

Appendix 1

Sample locations and petrographic description of the rocks studied by microprobe (cf. Tab. 1). All samples stored at ETH Zürich, Institut für Mineralogie und Petrographie.

Adamello samples (Italian coordinates)

For description of these skarns and adjacent rocks see CALLEGARI (1962), BRACK (1984), GROBETY (1985), and WERSIN (1985).

K1 (32TPR 1983 9712) Grey-green skarn belonging to the Buchenstein unit at the SE contact of the Adamello tonalite.
Fine-grained polygonal assemblage of gar-wo-qz-plag between the tonalite and a zone with wo-gar including patches containing wo-blades; Fig. 10.

K2 (32TPR 2165 9595) Same skarn unit as "K1", but coarser grained mosaic texture of gar-pla-qz-cc-dio; wo rare as relic in cc only; Fig. 12. Secondary epidote replacing plag and gar.

Bregaglia and Ticino samples (Swiss coordinates)

Calcic skarns with low variance assemblages around the Bregaglia intrusion are reported by various authors. Samples from three localities are reexamined here (Fig. 9): Val Sissone, Val Preda Rossa, and Val Schiesone.

Val Sissone sample (BUCHER, 1977):

Sis (776.76/129.57 coll. BUCHER) Equigranular, polygonal mosaic of wo-cc-gar-plag-dio with small amounts of qz.

Preda Rossa samples (ENGI, 1973):

PR 1 (774.54/122.13) Laminated nematoblastic texture of Wo-blades, platy qz, and sodic plag. Gar in vermicular aggregates between wo and plag-qz-rich layers. Interstitial Kspar, hydrogarnet, and vein-filling mica indicate some late alteration.

PR 2 (774.54/122.13) Equigranular wo-qz assemblage alternates with cc-rich bands. Gro as patchy prophyroblasts with Kspar, ido, and dio.

PR 3 (775.50/122.81) Mosaic texture of abundant wo and small amounts of qz, coexisting with large euhedral gar. Adjacent layers contain coarse cc with some gar and dio.

Val Schiesone sample (geological information in SCHMUTZ, 1976; TROMMSDORFF, 1966; petrology in OTERDOOM and GUNTER, 1983):

Sci (752.64/129.27 coll. TROMMSDORFF) Laminae of wo with cc, oligoclase, dio and poikiloblastic gar.

Ticino sample from Claro (TROMMSDORFF, 1968; CODONI, 1981):

Cla (723.262/123.927 coll. CODONI) Calcsilicate rock in regional Alpine amphibolite facies.
Mosaic of gra-qz-cc-plag-dio. Secondary clinozoisite and wo along veins.

Appendix 2

Analytical conditions

Mineral compositions were determined with an ARL SEMQ microprobe, equipped with six crystal X-ray spectrometers and an X-ray energy dispersive system. 15 kV acceleration voltage, 20 nA reference sample current on brass, 20 sec counting time were applied. Natural and synthetic oxides and silicate standards were used. The ZAF-correction program EMMA (SOMMERAUER and GUBSER, ETH Zürich) was applied.

Assuming all Fe to be ferric, garnet analyses were normalized to 12 cations (program written by P. ULMER, 1985) which nearly always yielded fully charge balanced formulae of ideal site occupancy, i.e. Fe enters almost entirely into the andradite component (Tab. 4).